

Interphoton burst recurrence times: Single cell analysis in freely flowing solutions

Cite as: Appl. Phys. Lett. **90**, 053904 (2007); <https://doi.org/10.1063/1.2435327>

Submitted: 14 November 2006 . Accepted: 21 December 2006 . Published Online: 02 February 2007

Joshua B. Edel, and Andrew J. deMello



View Online



Export Citation

ARTICLES YOU MAY BE INTERESTED IN

[Nanometric three-dimensional tracking of individual quantum dots in cells](#)

Applied Physics Letters **90**, 053902 (2007); <https://doi.org/10.1063/1.2437066>



Measure Ready
M91 FastHall™ Controller

A revolutionary new instrument
for complete Hall analysis

Lake Shore
CRYOTRONICS

Interphoton burst recurrence times: Single cell analysis in freely flowing solutions

Joshua B. Edel^{a)}

*Institute of Biomedical Engineering, Imperial College London, London, SW7 2AZ,
United Kingdom and Department of Chemistry, Imperial College London, London, SW7 2AZ,
United Kingdom*

Andrew J. deMello^{b)}

Department of Chemistry, Imperial College London, London, SW7 2AZ, United Kingdom

(Received 14 November 2006; accepted 21 December 2006; published online 2 February 2007)

The authors present a simple and direct analysis method for the discrimination between different cell populations in fluidic media. The methodology is based on analysis of single particle interphoton burst recurrence times and has potential use in high precision single cell sizing and counting applications. The approach requires registration of only a few hundred photons from single fluorescent particles to distinguish between different molecular populations. The technique is simple to implement and can be designed to extract information in real time within microfluidic environments. © 2007 American Institute of Physics. [DOI: [10.1063/1.2435327](https://doi.org/10.1063/1.2435327)]

Single molecule spectroscopy in solution is a relatively nascent field of research but has become increasingly applied to many contemporary chemical and biological problems.^{1–8} Over the past few years a number of techniques with sufficient sensitivity have been developed to detect single molecules in solution. Scanning probe microscopies (most notably scanning tunneling and atomic force microscopies) have been used to great effect in the analysis of surface bound species,⁹ but for the detection of single molecules in liquids optical methods incorporating the measurement of absorption and emission processes have proved most successful. The approach used herein for analyzing single cells in fluidic media integrates microfluidics with single molecule confocal fluorescence spectroscopy incorporating femtoliter detection volumes.

In order to assess the feasibility of interphoton burst recurrence times initial studies were focused on the detection of *Escherichia coli* (*E. coli*) cells expressed with various types of fluorescent proteins. The vast majority of confocal fluorescence spectroscopic experiments rely on binning photon burst scans into set intervals to allow observation of the number of fluorescence photons arriving in each time interval. Although this approach has proved to be valuable for single molecule fluorescence based experiments, more information can be obtained by registering and performing statistics on individual photon arrival times. A number of research groups have proposed a theoretical basis for the analysis of individual photon arrival times from single molecules.^{10–13} In this letter we present a technique that requires registration of a few hundred photons from single particles to distinguish between different molecular populations. This technique can potentially be used to size, sort, and distinguish between different particles or cells within a microfluidic channel with high precision and throughput.

A confocal spectrometer built in-house consisting of a 438 nm picosecond pulsed diode laser (PicoQuant GmbH) was used for all experiments and was described in detail elsewhere.⁵ A simple straight microfluidic channel design

consisting of one input and one output was used for all experiments and fabricated in glass using previously described methods.⁷ The microchannel was 60 μm wide, 20 mm long, and 30 μm deep. All samples were delivered hydrodynamically through the fluidic chip using a precision syringe pump (PHD 2000, Harvard Apparatus, Cambridge, MA).

Escherichia coli (*E. coli*) cells expressed with cyano, green, and yellow fluorescent proteins (CFP, GFP, and YFP) were synthesized according to the following procedure. *E. Coli*, strain BL21 Gold (DE3), containing the plasmid encoding fluorescent proteins (Living Colors™ range, Clontech, NJ) were grown to midlog phase in Luria-Bertani broth (LB medium) (1% tryptone, 1% NaCl, 0.5% Bacto yeast extract) containing 100 $\mu\text{g}/\text{ml}$ ampicillin at 37 °C with shaking. Cells were allowed to express the protein for approximately 16 h before harvesting by centrifugation at $3220\times g$ for 10 min at 4 °C. Cells were washed twice before resuspension to a final concentration of approximately 10^8 cells/ml.

An example of a single cell photon burst scan for *E. coli* expressed with GFP is shown in Fig. 1(a). Each burst above background threshold reports a single cell transversing the detection probe volume. The volumetric flow rates within the microfluidic channel were 2, 1, and 0.5 $\mu\text{l}/\text{min}$. The dwell time in all cases was set to 100 μs . The background threshold was determined to be 1.2 counts/bin and the average photon burst signal intensity for a flow rate of 2 $\mu\text{l}/\text{min}$ was 192 counts.

Significantly, variation of the fluorescent protein to either CFP or YFP within the *E. coli* cells results in entirely different burst characteristics when compared to GFP [Fig. 1(b)]. This effect arises due to the three fluorescent proteins having different absorption cross sections at 438 nm (excitation wavelength). CFP and GFP have absorption cross sections of approximately $5\times 10^3\text{ M}^{-1}\text{ cm}^{-1}$ while YFP has a cross section which is approximately 6 times lower. Secondly, burst height variations also originate from the fluorescent proteins having varying fluorescence quantum yields. The fluorescence quantum yields for CFP, GFP, and YFP are 0.4, 0.6, 0.7, respectively. For the acquisitions shown in Fig. 1(b), the average burst height for CFP was 127 counts with a relative standard deviation (RSD) of 117%. The dwell time

^{a)}Electronic mail: joshua.edel@imperial.ac.uk

^{b)}Electronic mail: a.demello@imperial.ac.uk

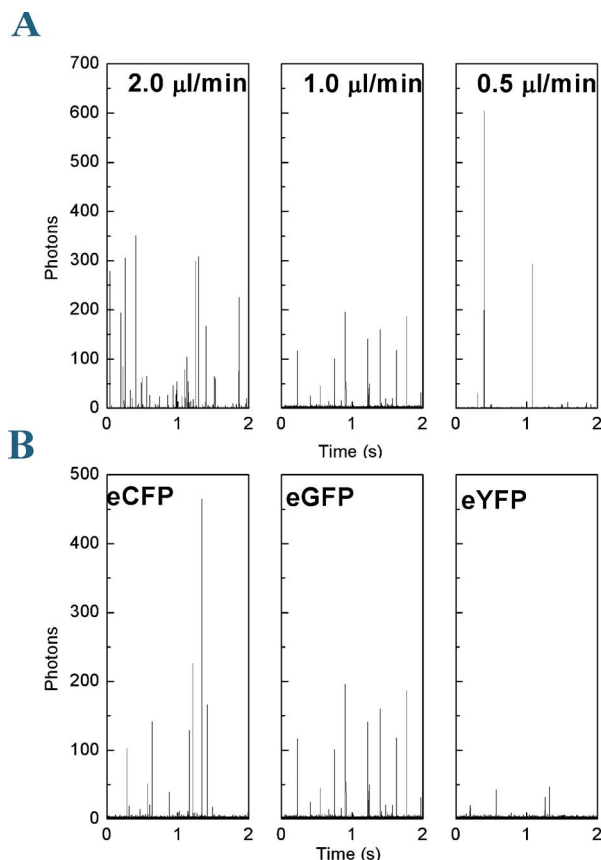


FIG. 1. (a) Representative single cell fluorescence burst scans for *E. coli* expressed with GFP. The volumetric flow rates (left to right) are 2, 1, and 0.5 $\mu\text{l}/\text{min}$, respectively. (b) Representative single cell fluorescence burst scans for *E. coli* expressed with CFP, GFP, and YFP (left to right). The volumetric flow rates in all the plots were 1.0 $\mu\text{l}/\text{min}$.

in all plots was 100 μs and the flow rate was constant at 1 $\mu\text{l}/\text{min}$. For GFP expressed cells under identical conditions, an average burst contained 80 counts and the RSD was 112%. In both cases these values were calculated from 500 bursts over a 65 s period. Burst statistics are significantly worse for YFP as a result of the low absorption cross section at 438 nm. A total of 200 bursts could be detected within a 65 s period at an identical cell concentration. The average burst height was 30 counts; however, the burst height deviation was reduced to a RSD of 85%. This is most likely a result of bursts being hidden in the background noise and as such, not being identified as bursts. The threshold in all burst scans was 3 ± 0.3 counts; hence the signal to noise ratio in YFP was typically not larger than 10.

A schematic of our interphoton burst recurrence time approach is shown in Fig. 2. A picosecond laser pulse train with a repetition rate of 10 MHz (100 ns spacing) is used to excite cells within the detection probe volume [Fig. 2(a)]. Once an analyte species is excited within the detection probe volume, molecular deexcitation can be achieved by either emission of a photon or via nonradiative relaxation mechanisms. Hence, a single laser pulse will not necessarily result in a photon being emitted. This can be described in terms of a two state system, and defines an “on” state if a photon is registered and an “off” state if no photon is registered for a given laser pulse. However, when a photon is registered its arrival time relative to the first excitation pulse is recorded. The acquisition card used for the current experiments (time-harp 100, PicoQuant GmbH) has a time resolution of 37 ps

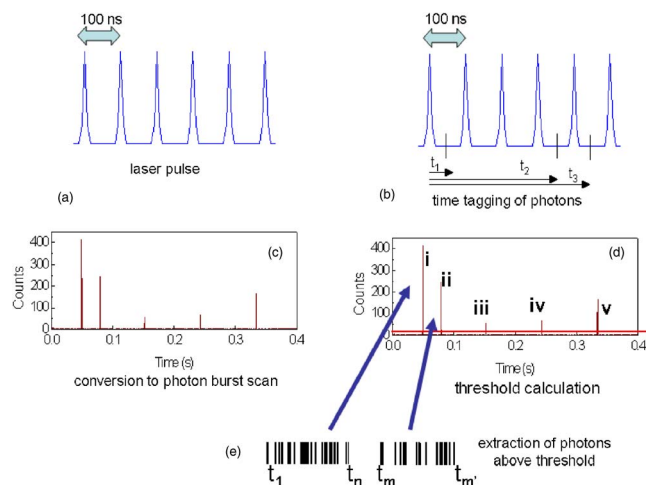


FIG. 2. (Color online) Schematic principle of the initial steps of an inter-photon burst recurrence time analysis.

and a dead time of 100 ns, thus a maximum of one photon can be registered from a single laser pulse within a 100 ns time window. Each photon is assigned its arrival time, t_1, t_2, \dots, t_n , as shown in Fig. 2(b). The time-tagged photons are then binned into predefined intervals to extract the cell photon burst scan, as shown in step Fig. 2(c). From this scan, the peaks are located and the background threshold is calculated. Since the background shot noise is expected to exhibit Poisson statistics, the early part of the photocount distribution can be modeled to a Poisson distribution which sets a statistical limit for the threshold. Photon counting events above this threshold can be defined as photon bursts associated with the presence of single cellular events. The selected peak discrimination threshold can be defined as three standard deviations from the mean background count rate, i.e.,

$$n_{\text{threshold}} = \mu + 3\sqrt{\mu}. \quad (1)$$

A threshold that lies three standard deviations above the mean background yields a confidence limit that is typically greater than 99%. All photons not associated with a photon burst or photons which are below the threshold are discarded [Fig. 2(d)]. The remaining time-tagged photons are extracted into “photon bar codes” [Fig. 2(e)] and analyzed by calculating the time difference between consecutive photon arrival times.

It will be shown that the photon bar codes for *E. coli* cells expressing different fluorescent proteins and fluorescent particles are distinguishable based upon a recurrence time analysis. The recurrence times are calculated as follows: \mathbf{P} is defined as a unit vector containing all times a photon burst is recorded [from Fig. 2(e)]. From this vector Δt is determined by taking the difference between all consecutive points in this vector, i.e., $R_i(i) = \mathbf{P}(i+1) - \mathbf{P}(i)$. The vector \mathbf{R}_i contains the complete list of time differences between consecutive photons for a photon burst scan. This is then histogrammed into bins with a resolution of 100 ns to obtain the interphoton burst recurrence frequency.

Examples of the normalized interphoton burst recurrence frequencies versus time for *E. coli* cells expressed with GFP are shown in Fig. 3. All curves are calculated from a photon burst scan containing a minimum of 1000 cells. The flow velocity through the microfluidic channel was varied between 0.5 and 5 $\mu\text{l}/\text{min}$. Two unique contributions arise from the interphoton burst frequency plots. The decay be-

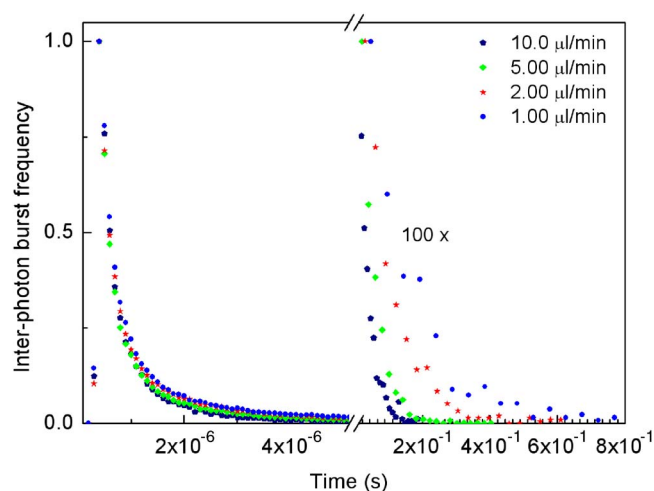


FIG. 3. (Color online) Normalized interphoton burst frequency for *E. coli* expressed with GFP. The first contribution (left) arises from photons associated with a single cellular event, the second from intracellular events.

tween 100 ns and 100 μ s is a result of a contribution arising from the photon arrival times associated with individual cellular events [equivalent to $t_n - t_{n-1}$ in Fig. 2(e)]. This contribution has no dependence on the velocity of the analyte through the detection probe volume. This is a result of the interburst frequency being strictly dependent on the total number of molecular events recorded per unit time. The second contribution between 10 ms and 1 s is a result of photon arrival times between different molecules [equivalent to $t_m - t_n$ in Fig. 2(e)]. This contribution is equivalent to a Poisson recurrence time analysis between individual cellular events.

Burst interval distributions are predicted to follow a Poissonian model, in which peak separation frequencies adopt an exponential form.^{5,14} This can clearly be seen if the second contribution is modeled to an exponential decay [Eq. (2)] describing the probability of a single cell event occurring after an interval Δt .

$$N(\Delta t) = \lambda \exp(-\beta t). \quad (2)$$

Here λ is a proportionality constant and β is a characteristic frequency at which single molecule events occur. The recurrence time τ_R can then be simply defined as

$$\tau_R = \frac{1}{\beta}. \quad (3)$$

For the current experiments, the recurrence time varies between 29 and 122 ms for flow velocities ranging from 1 to 10 μ l/min.

In Fig. 4 the first contributions of the interphoton burst frequency are shown for *E. coli* expressed with CFP, GFP, and YFP and modeled to a biexponential decay. The time constants and relative amplitudes are 267 ns (3.6) and 1.5 μ s (0.27) for CFP, 410 ns (1.9) and 1.7 μ s (0.35) for GFP and 854 ns (1.0) and 3.4 μ s (0.47) for YFP. The flow velocity through the microfluidic channel was set at 1 μ l/min and in all three cases a minimum of 1000 bursts were accumulated to calculate the decay. The distinct change in the decay profile for cells expressed with different proteins provides a simple method for distinguishing between different cellular populations without performing full fluorescence lifetime deconvolution. The differences in recovered decay constants

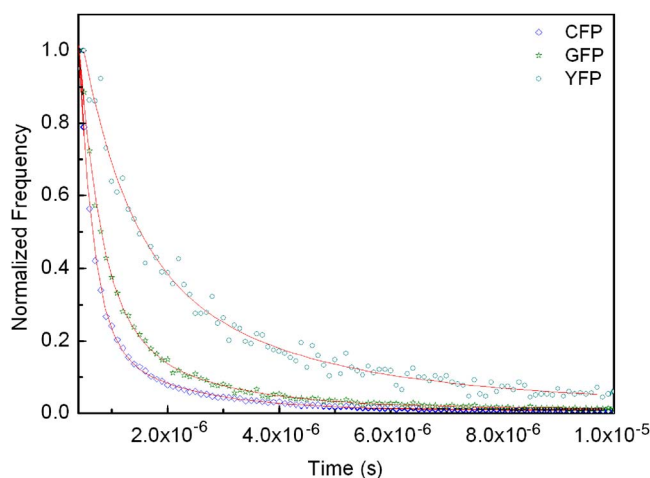


FIG. 4. (Color online) Normalized first contribution of the interphoton burst frequency for *E. coli* expressed with CFP, GFP, and YFP.

are largely due to differences in absorption cross sections and fluorescence quantum yields as well as the excitation and emission efficiencies. A large variation in these parameters will result in drastically different interphoton burst decays. This is clearly seen in Fig. 4 and indicates that this direct analysis method is an ideal approach for discriminating between fluorophores embedded within cells for “on-the-fly processing.” In principle, these experiments can be further extended to perform single cell recognition with the implementation of a maximum likelihood estimator algorithm. By integration of a multicolor detection system it would also be possible to perform multiplexed experiments where the simultaneous detection of different types of fluorescent protein would be possible.

In conclusion, this letter presents a technique that can be used to discriminate between different cell populations. The method uses single photon time tagging as well as interphoton burst times to allow species discrimination in a real-time fashion, and importantly, should have potential applications in single cell sizing and cell counting with high precision. The technique can also be used to determine event frequencies and flow velocities via the second contribution.

¹M. D. Barnes, W. B. Whitten, and J. M. Ramsey, *Anal. Chem.* **67**, 418A (1995).

²T. H. Wang, Y. H. Peng, C. Y. Zhang, P. K. Wong, and C. M. Ho, *J. Am. Chem. Soc.* **127**, 5354 (2005).

³S. M. Stavis, J. B. Edel, K. T. Samiee, and H. G. Craighead, *Lab Chip* **5**, 337 (2005).

⁴G. B. Lee, C. H. Lin, and S. C. Chang, *J. Micromech. Microeng.* **15**, 447 (2005).

⁵J. B. Edel, E. K. Hill, and A. J. de Mello, *Analyst (Cambridge, U.K.)* **126**, 1953 (2001).

⁶A. van Orden, R. A. Keller, and W. P. Ambrose, *Anal. Chem.* **72**, 37 (2000).

⁷J. B. Edel and A. J. de Mello, *Phys. Chem. Chem. Phys.* **5**, 3973 (2003).

⁸R. A. Keller, W. P. Ambrose, A. A. Arias, H. Gai, S. R. Emory, P. M. Goodwin, and J. H. Jett, *Anal. Chem.* **74**, 316A (2002).

⁹F. Vargas, O. Holtricher, O. Marti, G. de Schaetzen, and G. Tarrach, *J. Chem. Phys.* **117**, 866 (2002).

¹⁰T. Burzykowski, J. Szubiakowski, and T. Ryden, *Chem. Phys.* **288**, 291 (2003).

¹¹H. Yang and X. S. Xie, *J. Chem. Phys.* **117**, 10965 (2002).

¹²E. Novikov, J. Hofkens, M. Cotlet, M. Maus, F. C. De Schryver, and N. Boens, *Spectrochim. Acta, Part A* **57**, 2109 (2001).

¹³R. J. Cook and H. J. Kimble, *Phys. Rev. Lett.* **54**, 1023 (1985).

¹⁴M. A. Osborne, S. Balasubramanian, W. S. Furey, and D. Klenerman, *J. Phys. Chem. B* **102**, 3160 (1998).